MATCHED FIELD PROCESSING USING MULTIPOLE EXPANSION

Christoph F. Mecklenbräuker*[1] Andreas Waldhorst[1] Peter Gerstoft[2] and Georgios Haralabus[3]

[1]Signal Theory Group, Ruhr-University Bochum, D–44780 Germany
[2]Marine Physical Laboratory, Scripps Inst. Oceanography, CA 92093-0704 USA
[3]SACLANT Undersea Research Centre, La Spezia, I-19138 Italy

The underwater acoustic source field is expressed in terms of the multipole series which depends on source moments. This is a generalization of the monopole field representation which is used extensively in matched field processing. The generalization allows for acoustic sources with unknown higher-order moments. It is shown that including the dipole contribution into the source model may enhance the performance of matched field processing algorithms. Incorporating higher terms of the expansion leads to algorithms depending on spatial derivatives of the Green's function replica vector. The Green's function and its derivatives are computed using a normal-mode approach in this paper. The proposed approach is applied to acoustic data acquired with a towed array during a sea trial east of Bornholm in the Baltic Sea.

1. INTRODUCTION

Idealized monopoles in an ocean waveguide have been widely used for modeling acoustic sources in Matched Field Processing (MFP) algorithms [2, 4, 10, 5]. MFP uses replicas from the Green's function which are appropriate for both the coherence structure and the waveguide. Assuming a dipole source, however, leads to MFP algorithms which depend on spatial derivatives of the Green's function.

As far as the acoustic pressure outside the region of excitation is concerned, any acoustic source distribution may be replaced by a suitable collection of multipoles, cf. [13, 8]. The resulting series, *multipole expansion*, is redundant and strongly related to other expansions of the acoustic field. Seismic sources and ice cracks have been described using moments in the literature [1]. However, modeling of the ocean acoustic sources has mostly been limited to a monopole for matched field processing (one exception being surface generated noise [11, 7]). For near-field problems, it is to be expected that this is not a good approximation when the region of acoustic excitation spans several wavelengths.

Examples being shipping noise emitted from surface ships and submarines, earthquakes, and flow-noise in pipelines. Further, the asymptotic behavior of spatial Green's function derivatives in the far-field suggests that dipole and quadrupole moments are not negligible when compared to the fundamental monopole field contribution.

The region where this is of interest can be quite large as can be seen from the "Lloyd mirror effect" [9]. A (virtual) dipole is created by the sea surface due to a simple source

*now affiliated with SIEMENS AG Österreich, PSE TN MNR, Vienna, Austria in the water column. For a dipole in free space we will always get a zero field on the mid-plane between the two poles and a less fast decreasing field along the axis of the dipole. It is probably the interaction with inhomogeneous media and rough boundaries that destroys the higher-order multipole contribution to the acoustic field.

Green's theorem provides an integral formulation for underwater acoustic propagation [9]. The sound pressure X at sensor location $\mathbf{r}$ resulting from a source distribution S inside a volume $V_\circ$ is given by[1]

$$X(\mathbf{r};\omega) = \int_{V_\circ} G(\mathbf{r},\mathbf{u};\omega) S(\mathbf{u};\omega)\,\mathrm{d}^3u \ , \tag{1}$$

where we have ignored the boundary terms. For the moment, we select an arbitrary "source reference location" $\mathbf{r}_\circ \in V_\circ$, see Fig. 1. In the following, we will assume that the observation point $\mathbf{r}$ is *outside* the source volume $V_\circ$.

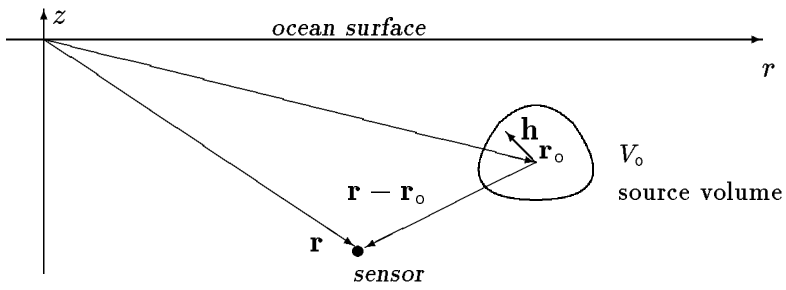

Figure 1: Geometry of acoustic excitation

The purpose of this paper is to show how the full multipole expansion can be used in MFP algorithms where mainly second-order statistics, i.e. the *cross spectral density*, of the signals are exploited. It turns out that usage of higher terms of the expansion lead to MFP algorithms which depend on spatial derivatives of the Green's function replica vector. Here, we used a normal-mode approach for numerical calculation.

2. MEAN SIGNAL AND SPECTRUM FROM MULTIPOLES

Let the source distribution S be modeled as a stochastic process with mean $\mathsf{E}\,S = \mu_\mathrm{s}(\mathbf{u};\omega)$ and cross spectral density $C_\mathrm{ss}(\mathbf{u}_1,\mathbf{u}_2;\omega)$. The mean acoustic field μ_x at location $\mathbf{r}$ resulting from the source distribution inside $V_\circ$ is obtained from Eq.(1)

$$\mu_\mathrm{x}(\mathbf{r};\omega) = \int_{V_\circ} G(\mathbf{r},\mathbf{u};\omega)\mu_\mathrm{s}(\mathbf{u};\omega)\,\mathrm{d}^3u \ . \tag{2a}$$

Ignoring additive noise originating from the outside of $V_\circ$, the acoustic cross-spectral density is given by

$$C_\mathrm{xx}(\mathbf{r}_1,\mathbf{r}_2;\omega) = \iint_{V_\circ} G(\mathbf{r}_1,\mathbf{u}_1;\omega) C_\mathrm{ss}(\mathbf{u}_1,\mathbf{u}_2;\omega) G^*(\mathbf{r}_2,\mathbf{u}_2;\omega)\,\mathrm{d}^3u_1\,\mathrm{d}^3u_2 \ . \tag{2b}$$

Let us assume that the dimensions of the source volume $V_\circ$ are small compared to variations of G (i.e. the wavelength): From now on, all source points $\mathbf{u} \in V_\circ$ are written

[1] The differential volume element at $\mathbf{u}$ is denoted by d^3u

as $\mathbf{u} = \mathbf{r}_\circ + \mathbf{h}$. The gradient vector of G with respect to the source coordinates $\mathbf{r}_\circ$ is denoted by $\mathbf{d}(\mathbf{r}, \mathbf{r}_\circ; \omega)$. Expanding the Green's function into a Taylor series at $\mathbf{r}_\circ$ yields the approximations[2]

$$\begin{aligned} \mu_{\mathrm{x}}(\mathbf{r}; \omega) &= \mathbf{w}'(\mathbf{r}, \mathbf{r}_\circ; \omega)\mathbf{m}_{\mathrm{S}}(\omega) && \text{(3a)} \\ C_{\mathrm{xx}}(\mathbf{r}_1, \mathbf{r}_2; \omega) &= \mathbf{w}^*(\mathbf{r}_1, \mathbf{r}_\circ; \omega)\mathbf{C}_{\mathrm{S}}(\omega)\mathbf{w}(\mathbf{r}_2, \mathbf{r}_\circ; \omega)\ , && \text{(3b)} \end{aligned}$$

with the definitions $\mathbf{w}(\mathbf{r}_n, \mathbf{r}_\circ; \omega) = \left(\ G(\mathbf{r}_n, \mathbf{r}_\circ; \omega),\ \ \mathbf{d}'(\mathbf{r}_n, \mathbf{r}_\circ; \omega)\ \right)'$,

$$\mathbf{m}_{\mathrm{S}}(\omega) = \begin{pmatrix} m_1 \\ \mathbf{m}_2 \end{pmatrix}, \quad \mathbf{C}_{\mathrm{S}}(\omega) = \begin{pmatrix} c_{11} & \mathbf{c}_{12}^* \\ \mathbf{c}_{12} & \mathbf{C}_{22} \end{pmatrix} . \tag{3c}$$

Here, we have defined

$$\begin{aligned} m_1 &= \int_{V_\circ} \mu_{\mathrm{s}}(\mathbf{u}; \omega)\, \mathrm{d}^3 u, && \text{“mean monopole signal” (4a)} \\ \mathbf{m}_2 &= \int_{V_\circ} (\mathbf{u} - \mathbf{r}_\circ)\mu_{\mathrm{s}}(\mathbf{u}; \omega)\, \mathrm{d}^3 u, && \text{“mean dipole signal” (4b)} \\ c_{11} &= \iint_{V_\circ} C_{\mathrm{ss}}(\mathbf{u}_1, \mathbf{u}_2; \omega)\, \mathrm{d}^3 u_1\, \mathrm{d}^3 u_2, && \text{“monopole power” (4c)} \\ \mathbf{c}_{12} &= \iint_{V_\circ} (\mathbf{u}_1 - \mathbf{r}_\circ) C_{\mathrm{ss}}(\mathbf{u}_1, \mathbf{u}_2; \omega)\, \mathrm{d}^3 u_1\, \mathrm{d}^3 u_2, && \text{“mono–/dipole cross power” (4d)} \\ \mathbf{C}_{22} &= \iint_{V_\circ} (\mathbf{u}_1 - \mathbf{r}_\circ)(\mathbf{u}_2 - \mathbf{r}_\circ)' C_{\mathrm{ss}}(\mathbf{u}_1, \mathbf{u}_2; \omega)\, \mathrm{d}^3 u_1\, \mathrm{d}^3 u_2, && \text{“di–/dipole cross power” (4e)} \end{aligned}$$

Thus, we can replace the true continuous distributions $\mu_{\mathrm{s}}(\mathbf{u}; \omega), C_{\mathrm{ss}}(\mathbf{u}_1, \mathbf{u}_2; \omega)$ inside the source volume $V_\circ$ by a collection of multipoles

$$\begin{aligned} \mu_{\mathrm{s}} &:= m_1 \delta(\mathbf{u} - \mathbf{r}_\circ) + \mathbf{m}_2' \dot{\delta}(\mathbf{u} - \mathbf{r}_\circ) + \ldots && \text{(5)} \\ C_{\mathrm{ss}} &:= c_{11} \delta(\mathbf{u}_1 - \mathbf{r}_\circ)\delta(\mathbf{u}_2 - \mathbf{r}_\circ) + \ldots && \text{(6)} \end{aligned}$$

where $\dot{\delta}(\mathbf{r})$ is the negative gradient of the Dirac pulse. In cartesian coordinates x, y, z, it is defined by $\dot{\delta}(\mathbf{r}) = -(\dot{\delta}(x)\delta(y)\delta(z),\ \delta(x)\dot{\delta}(y)\delta(z),\ \delta(x)\delta(y)\dot{\delta}(z))'$.

The linear field superposition applies to the random acoustic pressure $X(\mathbf{r}, \omega)$. Thus, the superposition principle carries over to the mean acoustic field $\mu_{\mathrm{x}}(\mathbf{r}; \omega)$: it is the sum over all mean signals from the individual multipoles. This is described by Eq.(3a). For the spectral power $C_{\mathrm{xx}}(\mathbf{r}_1, \mathbf{r}_2; \omega)$, we cannot generally add-up the individual powers of the multipoles because the statistics might be correlated. Therefore, a double sum is needed in the general case. This is described by the quadratic form Eq.(3b). If the statistics of the individual multipole signals are uncorrelated then $\mathbf{C}_{\mathrm{S}}(\omega)$ in Eq.(3b) reduces to a diagonal matrix. Two special cases are of interest in this paper:

Zero-mean dipole. Let $S(\mathbf{u}; \omega) = S(\omega)[\delta(\mathbf{u} - \mathbf{r}_{\circ 1}) - \delta(\mathbf{u} - \mathbf{r}_{\circ 2})]$ be a zero-mean dipole with $\mu_{\mathrm{s}} = 0$, $\sigma^2 = \mathsf{E}|S|^2$ and its root mean-square moment is given by $\mathbf{p} = (\mathbf{r}_{\circ 1} - \mathbf{r}_{\circ 2})\sigma$. Then, $\mu_{\mathrm{x}} = 0$, $c_{11} = 0$, $\mathbf{c}_{12} = \mathbf{0}$, and C_{xx} is given by Eq.(3b) with $\mathbf{C}_{22} = \mathbf{p}\mathbf{p}'$.

[2] $\mathbf{a}', \mathbf{a}^*$ denote the transpose and hermitian operations, respectively.

Cloud of uncorrelated monopoles. Let the volume $V_\circ$ be filled by a "cloud" of M zero-mean monopoles with individual powers C_m at locations $\mathbf{r}_\circ + \mathbf{h}_m$. Then, $\mu_{\mathrm{x}} = 0$ and C_{xx} is given by Eq.(3b) with

$$\mathbf{C}_\mathrm{S} = \sum_{m=1}^{M} C_m \begin{pmatrix} 1 & \mathbf{h}'_m \\ \mathbf{h}_m & \mathbf{h}_m \mathbf{h}'_m \end{pmatrix} \tag{7}$$

Each monopole contributes to $\mathbf{C}_\mathrm{S}$ with a rank-1 term. By estimating the rank of $\mathbf{C}_\mathrm{S}$ from the observed sound pressure outside of $V_\circ$ at $N \geq 4$ sensor positions, it is possible to decide whether $V_\circ$ is filled with one, two, three, or more sources.

3. LOG-LIKELIHOOD

We define an $(N \times 4)$-matrix transfer function $\mathbf{H}(\vartheta;\omega)$ which contains the rows $\mathbf{w}'(\mathbf{r}_n, \mathbf{r}_\circ;\omega)$ for $n = 1 \ldots N$ and ϑ is the vector of unknown variables. Thus, $\mathbf{H}(\vartheta;\omega)$ contains the Green's function and its spatial derivatives as elements. Its rank is denoted by R with $R \leq 4$. Let the acoustic sound pressure be sampled at N sensors located at $\mathbf{r}_1, \ldots, \mathbf{r}_N$ over time. The observed time series is partitioned into data stretches of duration T from which we estimate cross-spectral density matrices $\hat{\mathbf{C}}_{\underline{\mathrm{x}}}(\omega)$ for all ω of interest by a sample mean over periodograms [6, 12]. Further, $\mathbf{Q}(\vartheta;\omega)$ denotes an $(N \times R)$-matrix containing a unitary basis of the signal space in its columns. This can be obtained by orthogonalizing $\mathbf{H}(\vartheta;\omega)$ numerically. Then, the log-likelihood (up to an arbitrary constant) for a deterministic source with both mono– and dipole excitation in uncorrelated noise is very similar to the log-likelihood for R deterministic monopole sources and corresponds to incoherent addition of Bartlett power, cf. [3, 6]

$$L_1(\vartheta) = -\frac{1}{J}\sum_{j=1}^{J} \log\left[1 - \mathrm{tr}\,\mathbf{B}(\vartheta;\omega_j)\right], \quad \mathbf{B}(\vartheta;\omega) = \frac{\mathbf{Q}^*(\vartheta;\omega)\hat{\mathbf{C}}_{\underline{\mathrm{x}}}(\omega)\mathbf{Q}(\vartheta;\omega)}{\mathrm{tr}\,\hat{\mathbf{C}}_{\underline{\mathrm{x}}}(\omega)}. \tag{8a}$$

4. EXPERIMENT AND CONCLUSION

Some insight into the distribution of acoustic power $C_{\mathrm{xx}}(\mathbf{r},\mathbf{r};2\pi f_\circ) + |\mu_{\mathrm{x}}(\mathbf{r};2\pi f_\circ)|^2$ in a shallow ocean for monopole and dipole fields can be obtained from Fig. 2. In this figure, constant-power contours are shown on plane slices through the water column for both cases. The monopole power distribution (a) is cylindrically symmetric. The field shown in (b) is excited by a source with non-vanishing mono– and dipole moments. It shows a dominant horizontal axis of radiation which destroys the circular constant-power contours. For acoustic data acquisition with horizontal line arrays this might present an interesting issue.

The experimental site was located in the Bornholm Deep, east of Bornholm island in the Baltic Sea. Several sonar experiments were conducted by Atlas Elektronik (Bremen) during the cruise between October 3rd and 13th, 1983. A fifteen-element hydrophone array was towed by the surface ship *Walther von Ledebur* (inter-element spacing 2.56 m). A moving broadband source was given by the co-operating ship *Hans Bürkner*. Sound waves originating from at least two other ships can be detected using a broadband F–Test, see [12]. Here, we are interested in the signal stemming from the towing ship because it is nearest to the array. The towing ship is always located in endfire position with respect to the horizontal array (the partial derivative of the Green's function with respect to the source angle vanishes in this case). The source-depth and source-bearing were assumed to be known at $-5\,\mathrm{m}$ and $0°$, respectively. In this case, the only unknown is source range, $\vartheta = r_\circ$, and its nominal value is given by $450\,\mathrm{m}$.

Sampling frequency was $f_s = 1024\,\mathrm{Hz}$ after low-pass filtering with cut-off $f_c = 256\,\mathrm{Hz}$. We use a record of 10 minutes duration, divided into 150 stretches of $T = 4\,\mathrm{s} = 4096$ samples each. For the estimate $\hat{\mathbf{C}}_{\underline{\mathrm{x}}}(\omega)$, we averaged over $K = 16$ Fourier-transformed snapshots of length $0.25\,\mathrm{s}$ (corresponds to 256 samples).

We calculated $L_1(r_\circ)$ for $300\,\mathrm{m} \leq r_\circ \leq 600\,\mathrm{m}$ for all data-stretches and compared it to the monopole log-likelihood after scaling them to equal maximum value 1 for each time-step. The monopole log-likelihood is given by L_1 when restricting $\mathbf{H}(\vartheta, \omega)$ to its first column. Both results in Fig. 3 show considerable ambiguity. In the case of the monopole source model, the true source range, $450\,\mathrm{m}$, is masked by the ambiguity at $370\,\mathrm{m}$ due to mismatch in source depth. The dipole model suffers from environmental noise because the signal space has dimension $R > 1$. Therefore the corresponding gray-scale figure is much darker in this case. However, the true source range at $450\,\mathrm{m}$ is clearly visible. This is partly due to the tolerance of the dipole model to source-reference location mismatch as shown in Eq.(7). Errors in $\mathbf{r}_\circ$ lead to modified $\mathbf{C}_\mathrm{S}$ which is implicitly estimated by evaluating L_1

We conclude with the following remarks: Assuming acoustic sources with non-vanishing multipole moments leads to usage of spatial Green's function derivatives in replica vectors for MFP. The signal space belonging to a multipole source can have dimension greater than one. As a drawback, additional noise is captured in the widened signal space also. Robustness of the approach to nominal value mismatch in source depth is demonstrated with real data.

ACKNOWLEDGMENTS

We like to thank M. Siegel, Atlas Elektronik, for providing the data and F. Seifert, TU Vienna, for computational resources. We are indebted to L. Klinkenbusch and J.F. Böhme, Ruhr-University, for helpful comments.

REFERENCES

[1] K. Aki and P.G. Richards. *Quantitative Seismology: Theory and Methods*, vol. 1 & 2. W.H. Freeman & Co., San Francisco, (1980).

[2] A.B. Baggeroer, W.A. Kuperman, and P.N. Mikhalevsky. An overview on matched field methods in ocean acoustics. *IEEE J. Ocean. Eng.*, 18(4):401–424, (1993).

[3] J.F. Böhme. Statistical array signal processing of measured sonar and seismic data. In *Proc. SPIE 2563 Advanced Signal Processing Algorithms*, San Diego, July (1995).

[4] N.R. Chapman and K.S. Ozard. Matched field inversion for geoacoustic poperties of young oceanic crust. In O. Diachok, A. Caiti, P. Gerstoft, and H. Schmidt, editors, *Proc. of Full-field inversion methods in ocean and seismo-acoustics.* Kluwer, (1995).

[5] P. Gerstoft. Inversion of seismoacoustic data using genetic algorithms and *a posteriori* probability distributions. *J. Acoust. Soc. Am.*, 95(2):770–782, February (1994).

[6] P. Gerstoft and C.F. Mecklenbräuker. Ocean acoustic inversion with estimation of *a posteriori* probability distributions. *J. Acoust. Soc. Am.*, 104(7):(to appear), July (1998).

[7] Rachel M. Hamson. The theoretical responses of vertical and horizontal line arrays to wind-induced noise in shallow water. *J. Acoust. Soc. Am.*, 78(5):1702–1712, November (1985).

[8] J.D. Jackson. *Classical Electrodynamics.* John Wiley & Sons, New York, 2nd edition, (1962).

[9] F.B. Jensen, W.A. Kuperman, M.B. Porter, and H. Schmidt. *Computational Ocean Acoustics.* American Institute of Physics Press, New York, (1994).

[10] S.M. Jesus. Broadband matched field processing of transient signals in shallow water. *J. Acoust. Soc. Am.*, 93(4):1841–1850, April (1993).

[11] W.A. Kuperman and F. Ingenito. Spatial correlation of surface generated noise in a stratified ocean. *J. Acoust. Soc. Am.*, 67(6):1988–1996, June (1980).

[12] C.F. Mecklenbräuker, D. Maiwald, and J.F. Böhme. F-test in matched field processing: Identifying multimode propagation. In *Proc. IEEE ICASSP*, pages 3123–3126, Detroit, May 8-12 (1995). IEEE.

[13] P.M. Morse and H. Feshbach. *Methods of Theoretical Physics.* McGraw-Hill, New York, (1953).

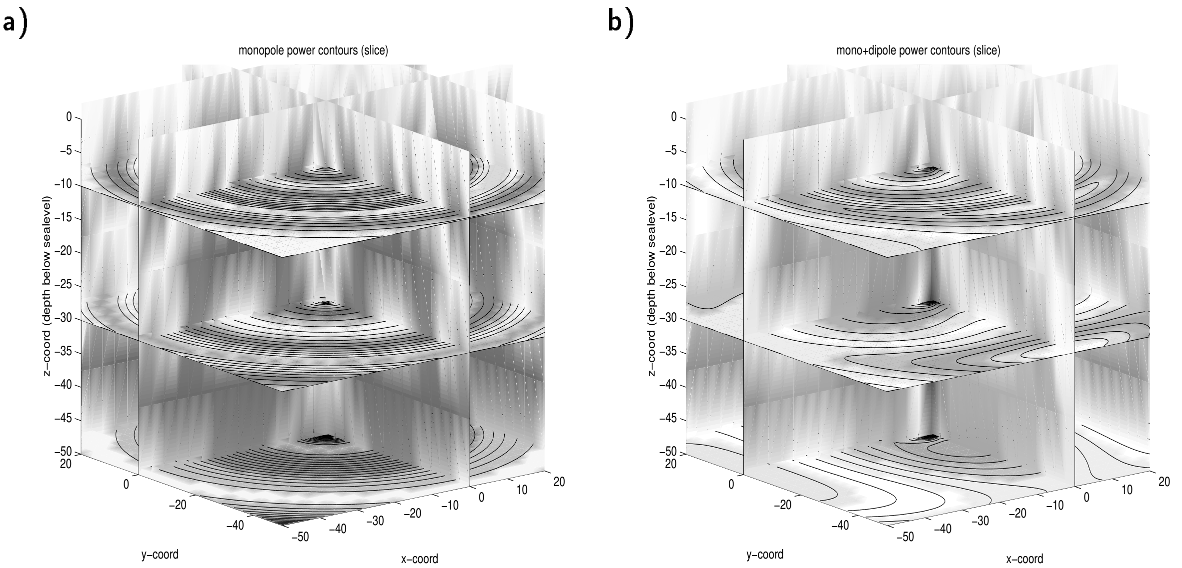

Figure 2: Equipower contours on slices through water column. Parameters: ocean depth 56 m, sound speed 1480 m/s, frequency $f_{\circ} = 50\,\text{Hz}$, source depth 5 m.

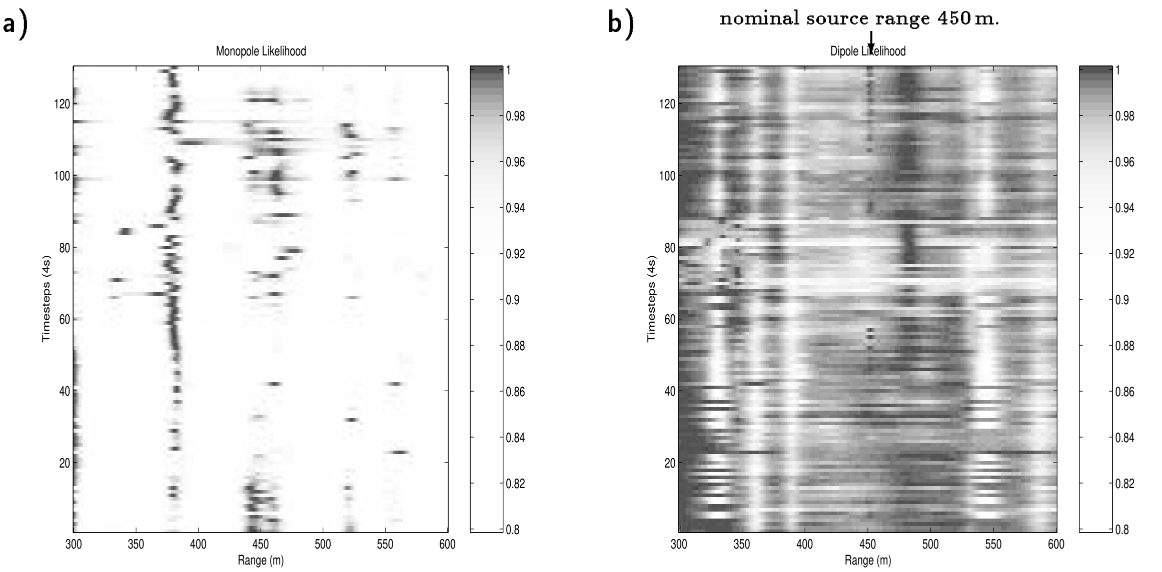

Figure 3: Grayscale plot of normalized log-likelihood for Bornholm data.